

Stochastic optimal control analysis of a piezoelectric shell subjected to stochastic boundary perturbations

Z.G. Ying^{*1}, J. Feng¹, W.Q. Zhu¹ and Y.Q. Ni²

¹Department of Mechanics, School of Aeronautics and Astronautics, Zhejiang University, Hangzhou 310027, P. R. China

²Department of Civil and Structural Engineering, The Hong Kong Polytechnic University, Kowloon, Hong Kong

(Received November 19, 2010, Revised December 22, 2011, Accepted February 20, 2012)

Abstract. The stochastic optimal control for a piezoelectric spherically symmetric shell subjected to stochastic boundary perturbations is constructed, analyzed and evaluated. The stochastic optimal control problem on the boundary stress output reduction of the piezoelectric shell subjected to stochastic boundary displacement perturbations is presented. The electric potential integral as a function of displacement is obtained to convert the differential equations for the piezoelectric shell with electrical and mechanical coupling into the equation only for displacement. The displacement transformation is constructed to convert the stochastic boundary conditions into homogeneous ones, and the transformed displacement is expanded in space to convert further the partial differential equation for displacement into ordinary differential equations by using the Galerkin method. Then the stochastic optimal control problem of the piezoelectric shell in partial differential equations is transformed into that of the multi-degree-of-freedom system. The optimal control law for electric potential is determined according to the stochastic dynamical programming principle. The frequency-response function matrix, power spectral density matrix and correlation function matrix of the controlled system response are derived based on the theory of random vibration. The expressions of mean-square stress, displacement and electric potential of the controlled piezoelectric shell are finally obtained to evaluate the control effectiveness. Numerical results are given to illustrate the high relative reduction in the root-mean-square boundary stress of the piezoelectric shell subjected to stochastic boundary displacement perturbations by the optimal electric potential control.

Keywords: piezoelectric shell; stochastic vibration; optimal control; boundary perturbation; stochastic response

1. Introduction

Piezoelectric structures as smart sensors or controllers have a potential application in engineering (Rao and Sunar 1994), for instance, to structural health monitoring (Park *et al.* 2005, Li and Zhang 2008), structural damage detection (Yu and Giurgiutiu 2005, Tawie *et al.* 2010), geotechnical engineering (Zeng 2006), and structural vibration control (Rudolf *et al.* 2010, Jin *et al.* 2010). The dynamic characteristics of piezoelectric and composite structures such as beam, plate and shell have been studied analytically and numerically (Saravanos and Heyliger 1999, Tzou and Zhong 1994, Ying *et al.* 2011). In smart piezoelectric structures, the piezoelectric shell structure has better electrical and

*Corresponding author, Professor, E-mail: yingzg@zju.edu.cn

mechanical coupling properties. The piezoelectric sensors and controllers have been applied to the vibration control (Balamurugan and Narayanan 2001, Tzou *et al.* 2002, Correia *et al.* 2002, Ray 2003, Trajkov *et al.* 2006, Huang and Tseng 2008, Sohn *et al.* 2009, Sheng and Wang 2009, Gupta *et al.* 2004) and acoustic control (Scandrett 2002, Li *et al.* 2004, Hasheminejad and Rajabi 2008) of shell structures. The linear feedback control strategy is used generally except neural network and genetic algorithms (Kumar *et al.* 2008, Roy and Chakraborty 2009).

In particular, the deterministic dynamic characteristics of piezoelectric shells have been studied extensively. The studies on piezoelectric cylindrical shells include the free vibration of piezoelectric ceramic cylinders radially polarized (Adelman *et al.* 1975, Ding *et al.* 2002, Berg *et al.* 2004), the torsional wave motion of a finite inhomogeneous piezoelectric cylindrical shell (Sarma 1980), the axisymmetric and other electroelastic waves of hollow piezoelectric ceramic cylinders (Shul'ga *et al.* 1984, Paul and Venkatesan 1987), and the transient response of axisymmetric piezoelectric hollow cylinders in plane strain analyzed by using the series expansion of Bessel functions and the linear interpolation algorithm (Ding *et al.* 2003, Babaev *et al.* 1990). The corresponding studies on the free and forced vibrations of piezoelectric spherical shells were also presented (Heyliger and Wu 1999, Chen *et al.* 2001, Loza and Shul'ga 1990, Li *et al.* 2000, Borisyuk and Kirichok 1979, Ding *et al.* 2003). Recently, the electro-elastic wave propagation in piezoceramic cylinders of sector cross-sections has been studied (Puzyrev 2010). Several studies on the stochastic dynamics of piezoelectric structures have been presented. The numerical analysis of shell structures with distributed piezoelectric control components was made by using the finite element method (Narayanan and Balamurugan 2003, To and Chen 2007). The theoretical solution approach to the stochastic response of piezoelectric axisymmetric hollow cylinders subjected to random boundary pressure and/or electric potential excitations was proposed and extended (Ying *et al.* 2009, Ying and Zhu 2009). However, the stochastic optimal control of piezoelectric shells under stochastic boundary perturbations remains and needs to be studied further, for instance, in improving the piezoelectric sensor capability against perturbations.

The present paper focuses on the stochastic optimal control analysis of a piezoelectric shell under stochastic boundary displacement perturbations. Firstly, the basic formulations of the spherically symmetric piezoelectric shell subjected to boundary displacement perturbations as well as the optimal control performance index are given. The stochastic optimal control problem on the boundary stress output reduction of the piezoelectric shell subjected to stochastic boundary perturbations is formed. Secondly, the electric potential is expressed as a function of displacement by integrating the electrostatics equation, and the differential equations for the piezoelectric shell with electrical and mechanical coupling are converted into the differential equation only for displacement. Then the stochastic boundary conditions are converted into homogeneous ones by using the constructed displacement transformation. The transformed displacement is expanded in space into a series, and the partial differential equation for displacement is converted further into ordinary differential equations according to the Galerkin method, which represent a multi-degree-of-freedom dynamic system with asymmetric stiffness matrix under stochastic excitations. Therefore the stochastic optimal control problem of the piezoelectric shell in partial differential equations is transformed into that of the multi-degree-of-freedom system in ordinary differential equations. Thirdly, the Hamilton-Jacobi-Bellman equation for the control system with performance index is presented according to the stochastic dynamical programming principle. The optimal control law for electric potential and the corresponding Riccati equation are determined in terms of the optimal regulation. Fourthly, the frequency-response function matrix, power spectral density matrix and correlation function matrix of the controlled system response are derived successively based on the theory of random vibration. The expressions of mean-

square stress, displacement and electric potential of the controlled piezoelectric shell are obtained for non-white stochastic perturbations, which are compared with the corresponding uncontrolled ones to evaluate the control effectiveness. Finally, numerical results are given to illustrate the stochastic stress, displacement and electric-potential responses of the controlled and uncontrolled piezoelectric shells to stochastic boundary displacement perturbations, the control effectiveness or relative reduction in the root-mean-square boundary stress and the corresponding optimal electric potential control input, and those varying with structure and excitation parameters.

2. Stochastic optimal control problem of a piezoelectric shell

The differential equations for piezoelectric shells with random boundary stress and electric potential excitations have been given (Ying and Zhu 2009). For a spherically symmetric piezoelectric shell, its differential equation of motion and charge equation of electrostatics in the radius r direction can be expressed as

$$\frac{\partial \sigma_{rr}}{\partial r} + 2 \frac{\sigma_{rr} - \sigma_{\theta\theta}}{r} = \rho \frac{\partial^2 u_r}{\partial t^2} + c_r \frac{\partial u_r}{\partial t} \quad (1)$$

$$\frac{1}{r^2} \frac{\partial}{\partial r} (r^2 D_r) = 0 \quad (2)$$

where $\sigma_{rr} = \sigma_{rr}(r, t)$ and $\sigma_{\theta\theta} = \sigma_{\theta\theta}(r, t)$ are respectively the radial and circular stresses, $u_r = u_r(r, t)$ is the radial displacement, ρ and c_r are respectively the mass density and damping coefficient, $D_r = D_r(r, t)$ is the radial electric displacement. The electric potential control is inputted by the shell surfaces, and then expressed by boundary conditions. The constitutive relations of orthotropic and radially polarized piezoelectric medium are

$$\sigma_{\theta\theta} = (c_{11} + c_{12})\gamma_{\theta\theta} + c_{13}\gamma_{rr} + e_{31} \frac{\partial \Phi}{\partial r} \quad (3a)$$

$$\sigma_{rr} = 2c_{13}\gamma_{\theta\theta} + c_{33}\gamma_{rr} + e_{33} \frac{\partial \Phi}{\partial r} \quad (3b)$$

$$D_r = 2e_{31}\gamma_{\theta\theta} + e_{33}\gamma_{rr} - \epsilon_{33} \frac{\partial \Phi}{\partial r} \quad (3c)$$

where $\gamma_{\theta\theta}$ and γ_{rr} are respectively the circular and radial strains, c_{ij} , e_{ij} and ϵ_{ij} ($i, j=1,2,3$) are respectively elastic, piezoelectric and dielectric constants, and $\Phi = \Phi(r, t)$ is the electric potential. The strain-displacement relations for the spherically symmetric problem are

$$\gamma_{rr} = \frac{\partial u_r}{\partial r}, \gamma_{\theta\theta} = \frac{u_r}{r} \quad (4a,b)$$

and the other displacement in spherical coordinates $u_\theta = 0$. The boundary conditions for displacements and stresses are given by

$$u_r(a, t) = u_{ra}(t), \sigma_{rr}(a, t) = p_{aa}(t) \quad (5a,b)$$

$$u_r(b, t) = u_{rb}(t), \sigma_{rr}(b, t) = p_{ba}(t) \quad (5c,d)$$

where a and b are respectively the inner and outer radii of the spherical shell, u_{ra} and u_{rb} are boundary displacements including stochastic perturbation and non-perturbation parts, p_{aa} and p_{ba} are boundary stresses with the perturbation part to be controlled. The electric potential consists of control and non-control parts, and the control part corresponds to minimizing the perturbation stresses induced by perturbation displacements. Then the boundary electric potentials are expressed by two parts as

$$\Phi(a, t) = \Phi_{aa}(t) + \Phi_{ca}(t), \quad \Phi(b, t) = \Phi_{ba}(t) + \Phi_{cb}(t) \quad (6a,b)$$

Separate the mechanical displacement, electric displacement and electric potential of the piezoelectric shell into two parts corresponding to non-control and control (or perturbation) as follows

$$u_r = u_a + u_r^s, \quad D_r = D_a + D_r^s, \quad \Phi = \Phi_a + \Phi^s \quad (7a,b,c)$$

where subscript “ a ” and superscript “ s ” denote non-control and control, respectively. Substituting Eq. (7) into Eqs. (1)-(4) and eliminating non-control parts yield equations for control parts

$$\frac{\partial \sigma_{rr}^s}{\partial r} + 2 \frac{\sigma_{rr}^s - \sigma_{\theta\theta}^s}{r} = \rho \frac{\partial^2 u_r^s}{\partial t^2} + c_r \frac{\partial u_r^s}{\partial t} \quad (8)$$

$$\frac{1}{r^2} \frac{\partial}{\partial r} (r^2 D_r^s) = 0 \quad (9)$$

$$\sigma_{\theta\theta}^s = (c_{11} + c_{12}) \frac{u_r^s}{r} + c_{13} \frac{\partial u_r^s}{\partial r} + e_{31} \frac{\partial \Phi^s}{\partial r} \quad (10a)$$

$$\sigma_{rr}^s = 2c_{13} \frac{u_r^s}{r} + c_{33} \frac{\partial u_r^s}{\partial r} + e_{33} \frac{\partial \Phi^s}{\partial r} \quad (10b)$$

$$D_r^s = 2e_{31} \frac{u_r^s}{r} + e_{33} \frac{\partial u_r^s}{\partial r} - \epsilon_{33} \frac{\partial \Phi^s}{\partial r} \quad (10c)$$

The corresponding boundary conditions are

$$u_r^s(a, t) = u_{ra}(t), \quad \Phi^s(a, t) = \Phi_{ca}(t) \quad (11a,b)$$

$$u_r^s(b, t) = u_{rb}(t), \quad \Phi^s(b, t) = \Phi_{cb}(t) \quad (11c,d)$$

where Φ_{ca} and Φ_{cb} are electric potential control inputs. The objective of stochastic optimal control is to minimize boundary stress components $\sigma_{rr}^s(a, t)$ and $\sigma_{rr}^s(b, t)$ induced by stochastic boundary displacement perturbations u_{ra} and u_{rb} . The performance index can be expressed as

$$J = E \left[\int_{t_0}^{t_f} \{ \alpha_1 \sigma_{rr}^s(a, t)^2 + \alpha_2 \sigma_{rr}^s(b, t)^2 \} dt \right] \quad (12)$$

where $E[\cdot]$ denotes the expectation operation, t_0 and t_f are respectively the initial and terminal times, α_1 and α_2 are weighting constants. Rewrite Eqs. (8)-(10) in the dimensionless form as follows

$$\frac{\partial \sigma_r}{\partial \lambda} + 2 \frac{\sigma_r - \sigma_\theta}{\lambda} = \frac{\partial^2 v}{\partial \tau^2} + c \frac{\partial v}{\partial \tau} \quad (13)$$

$$\frac{1}{\lambda^2} \frac{\partial}{\partial \lambda} (\lambda^2 D) = 0 \quad (14)$$

$$\sigma_\theta = c_1 \frac{v}{\lambda} + c_3 \frac{\partial v}{\partial \lambda} + e_1 \frac{\partial \phi}{\partial \lambda} \quad (15a)$$

$$\sigma_r = 2c_3 \frac{v}{\lambda} + \frac{\partial v}{\partial \lambda} + e_3 \frac{\partial \phi}{\partial \lambda} \quad (15b)$$

$$D = 2e_1 \frac{v}{\lambda} + e_3 \frac{\partial v}{\partial \lambda} - \frac{\partial \phi}{\partial \lambda} \quad (15c)$$

where

$$\begin{aligned} \sigma_i &= \frac{\sigma_{ii}^s}{c_{33}} \quad (i=r, \theta), \quad v = \frac{u_r^s}{b}, \quad D = \frac{D_r^s}{\sqrt{c_{33} \varepsilon_{33}}}, \quad \phi = \frac{\Phi^s}{b} \sqrt{\varepsilon_{33}} \\ \lambda &= \frac{r}{b}, \quad \tau = \frac{t}{b} \sqrt{\frac{c_{33}}{\rho}}, \quad c = \frac{bc_r}{\sqrt{\rho c_{33}}}, \quad c_1 = \frac{c_{11} + c_{12}}{c_{33}}, \quad c_3 = \frac{c_{13}}{c_{33}} \\ e_1 &= \frac{e_{31}}{\sqrt{c_{33} \varepsilon_{33}}}, \quad e_3 = \frac{e_{33}}{\sqrt{c_{33} \varepsilon_{33}}} \end{aligned} \quad (16)$$

The boundary conditions Eq. (11) becomes correspondingly

$$v(s, \tau) = \xi_a(\tau) = u_{ra}/b, \quad v(1, \tau) = \xi_b(\tau) = u_{rb}/b \quad (17a,b)$$

$$\phi(s, \tau) = U_a(\tau) = \frac{u_{ca}}{b} \sqrt{\frac{\varepsilon_{33}}{c_{33}}}, \quad \phi(1, \tau) = U_b(\tau) = \frac{u_{cb}}{b} \sqrt{\frac{\varepsilon_{33}}{c_{33}}} \quad (18a,b)$$

where $s = a/b$, U_a and U_b are controls, $\xi_a(t)$ and $\xi_b(t)$ are the stochastic processes with power spectral densities $S_{\xi_a}(\omega)$ and $S_{\xi_b}(\omega)$, respectively. The performance index Eq. (12) for control becomes as

$$J = E \left[\int_{\tau_0}^{\tau_f} \{ \alpha_1 \sigma_r(s, \tau)^2 + \alpha_2 \sigma_r(1, \tau)^2 \} d\tau \right] \quad (19)$$

Eqs. (13)-(15) and Eqs. (17)-(19) constitute a stochastic optimal control problem of the piezoelectric shell subjected to stochastic boundary displacement perturbations. The optimal control law can be determined by converting the partial differential control problem into an ordinary differential control problem.

3. Multi-degree-of-freedom control system

The stochastic optimal control problem for the piezoelectric shell in partial differential Eqs. (13)-(19) can be converted into that of a multi-degree-of-freedom system in ordinary differential equations.

3.1 Electric potential integral

By substituting electric displacement Eq. (15(c)) into Eq. (14), integrating this equation with respect to λ and using conditions Eq. (18), the electric potential ϕ is expressed by displacement v as

follows

$$\phi = 2e_1 \int_s^\lambda \frac{v}{\lambda} d\lambda + e_3(v - \bar{v}_a) + \frac{s-\lambda}{\lambda(1-s)} [2e_1 \int_s^\lambda \frac{v}{\lambda} d\lambda + e_3(\bar{v}_b - \bar{v}_a)] + \frac{1}{\lambda(1-s)} [s(1-\lambda)U_a + (\lambda-s)U_b] \quad (20)$$

where boundary displacements

$$\bar{v}_a = v(s, \tau), \quad \bar{v}_b = v(1, \tau) \quad (21a,b)$$

Substituting electric potential Eq. (20) and stresses Eq. (15) into Eq. (13) yields the differential equation of motion only for displacement v

$$(1+e_3^2) \frac{\partial^2 v}{\partial \lambda^2} + \frac{2(1+e_3^2)}{\lambda} \frac{\partial v}{\partial \lambda} - 2(c_1 - c_3 + 2e_1^2 - e_1 e_3) \frac{v}{\lambda^2} + \frac{4e_1^2 s}{\lambda^3(1-s)} \int_s^\lambda \frac{v}{\lambda} d\lambda - \frac{2e_1 e_3 s}{\lambda^3(1-s)} (\bar{v}_a - \bar{v}_b) + \frac{2e_1 s}{\lambda^3(1-s)} (U_a - U_b) = \frac{\partial^2 v}{\partial \tau^2} + c \frac{\partial v}{\partial \tau} \quad (22)$$

The corresponding boundary conditions are the same as Eq. (17). The radial stress Eq. (15(b)) becomes correspondingly

$$\sigma_r = (1+e_3^2) \frac{\partial v}{\partial \lambda} + 2(c_3 + e_1 e_3) \frac{v}{\lambda} - \frac{2e_1 e_3 s}{\lambda^2(1-s)} \int_s^\lambda \frac{v}{\lambda} d\lambda + \frac{e_3^2 s}{\lambda^2(1-s)} (\bar{v}_a - \bar{v}_b) - \frac{e_3 s}{\lambda^2(1-s)} (U_a - U_b) \quad (23)$$

The electrical and mechanical coupling problem [Eqs. (13)-(15) with Eqs. (17) and (18)] has been converted into a mechanical dynamics problem [Eqs. (22) and (17)].

3.2 Displacement transformation

To convert the stochastic boundary conditions [Eq. (17)] into homogeneous ones and expand the displacement as a series in radial functions, the following displacement transformation is introduced firstly

$$v = -\frac{\lambda-1}{1-s} \xi_a + \frac{\lambda-s}{1-s} \xi_b + v_0 \quad (24)$$

By the substitution of transformation Eq. (24) into Eq. (17), the boundary conditions for displacement component v_0 obtained are

$$v_0(s, \tau) = 0, \quad v_0(1, \tau) = 0 \quad (25a,b)$$

Substituting transformation Eq. (24) into Eq. (22) yields the differential equation for displacement v_0 as follows

$$\begin{aligned} \frac{\partial^2 v_0}{\partial \tau^2} + c \frac{\partial v_0}{\partial \tau} = & (1+e_3^2) \frac{\partial^2 v_0}{\partial \lambda^2} + \frac{2(1+e_3^2)}{\lambda} \frac{\partial v_0}{\partial \lambda} - 2(c_1 - c_3 + 2e_1^2 - e_1 e_3) \frac{v_0}{\lambda^2} + \frac{4e_1^2 s}{\lambda^3(1-s)} \int_s^\lambda \frac{v_0}{\lambda} d\lambda \\ & + \left[-\frac{2(1+e_3^2)}{\lambda(1-s)} + 2(c_1 - c_3 + 2e_1^2 - e_1 e_3) \frac{\lambda-1}{\lambda^2(1-s)} - \frac{4e_1^2 s}{\lambda^3(1-s)^2} (1-s + \ln s) - \frac{2e_1 e_3 s}{\lambda^3(1-s)} \right] \xi_a \\ & + \left[\frac{2(1+e_3^2)}{\lambda(1-s)} - 2(c_1 - c_3 + 2e_1^2 - e_1 e_3) \frac{\lambda-s}{\lambda^2(1-s)} + \frac{4e_1^2 s}{\lambda^3(1-s)^2} (1-s + s \ln s) + \frac{2e_1 e_3 s}{\lambda^3(1-s)} \right] \xi_b \\ & + \frac{\lambda-1}{1-s} \left(\frac{\partial^2 \xi_a}{\partial \tau^2} + c \frac{\partial \xi_a}{\partial \tau} \right) - \frac{\lambda-s}{1-s} \left(\frac{\partial^2 \xi_b}{\partial \tau^2} + c \frac{\partial \xi_b}{\partial \tau} \right) + \frac{2e_1 s}{\lambda^3(1-s)} (U_a - U_b) \end{aligned} \quad (26)$$

The radial stress Eq. (23) becomes correspondingly

$$\begin{aligned}
 \sigma_r = & (1 + e_3^2) \frac{\partial v_0}{\partial \lambda} + 2(c_3 + e_1 e_3) \frac{v_0}{\lambda} - \frac{2e_1 e_3 s}{\lambda^2 (1-s)} \int_s^1 \frac{v_0}{\lambda} d\lambda \\
 & + \left[-\frac{1 + e_3^2}{1-s} - 2(c_3 + e_1 e_3) \frac{\lambda - 1}{\lambda(1-s)} + \frac{2e_1 e_3 s}{\lambda^2 (1-s)^2} (1-s + \ln s) + \frac{e_3^2 s}{\lambda^2 (1-s)} \right] \xi_a \\
 & + \left[\frac{1 + e_3^2}{1-s} + 2(c_3 + e_1 e_3) \frac{\lambda - s}{\lambda(1-s)} - \frac{2e_1 e_3 s}{\lambda^2 (1-s)^2} (1-s + s \ln s) - \frac{e_3^2 s}{\lambda^2 (1-s)} \right] \xi_b \\
 & - \frac{e_3 s}{\lambda^2 (1-s)} (U_a - U_b)
 \end{aligned} \tag{27}$$

3.3 Galerkin method

The displacement v_0 is then expanded in the radial coordinate as follows

$$v_0(\lambda, \tau) \approx \sum_{j=1}^n q_j(\tau) \sin \frac{\lambda - s}{1-s} j\pi \tag{28}$$

where $q_j(\tau)$ is a function of time, representing the modal displacement. Obviously, displacement Eq. (28) satisfies the homogeneous boundary conditions Eq. (25). According to the Galerkin method, substituting displacement Eq. (28) into Eq. (26), multiplying this equation by $\sin i\pi(\lambda-s)/(1-s)$ and integrating it with respect to λ on $[s, 1]$ yield ordinary differential equations for $q_j(\tau)$, which can be rewritten in the following matrix form

$$\ddot{\mathbf{Q}} + \mathbf{C}\dot{\mathbf{Q}} + \mathbf{K}\mathbf{Q} = \mathbf{F}(\tau) + \mathbf{B}U \tag{29}$$

where the superscript “.” denotes the derivative with respect to τ , modal displacement vector $\mathbf{Q} = [q_1, q_2, \dots, q_n]^T$, modal damping matrix $\mathbf{C} = \text{diag}[c]$, electric potential control input $U = U_a - U_b$, and modal stiffness matrix \mathbf{K} , modal stochastic excitation vector \mathbf{F} and modal control coefficient vector \mathbf{B} have elements respectively

$$K_{ij} = \frac{(1 + e_3^2)}{(1-s)^2} (i^2 \pi^2 \delta_{ij} - 2j\pi a_{1ij}) + \frac{2(c_1 - c_3 + 2e_1^2 - e_1 e_3)}{1-s} a_{2ij} - \frac{8e_1^2 s}{(1-s)^2} b_{3i} b_{1j} \tag{30a}$$

$$F_i(\tau) = C_{1i} \xi_a(\tau) + D_{1i} \xi_b(\tau) + C_{2i} \dot{\xi}_a(\tau) + D_{2i} \dot{\xi}_b(\tau) + C_{3i} \ddot{\xi}_a(\tau) + D_{3i} \ddot{\xi}_b(\tau) \tag{30b}$$

$$B_i = \frac{4e_1 s}{(1-s)} b_{3i} \tag{30c}$$

in which $\delta_{ii} = 1$ and $\delta_{ij} = 0$ ($i \neq j$)

$$C_{1i} = -\frac{4(1 + e_3^2)}{(1-s)^2} b_{1i} + \frac{4(c_1 - c_3 + 2e_1^2 - e_1 e_3)}{(1-s)^2} (b_{1i} - b_{2i}) - \frac{4e_1 e_3 s}{(1-s)^2} b_{3i} - \frac{8e_1^2 s(1-s + \ln s)}{(1-s)^3} b_{3i}$$

$$D_{1i} = \frac{4(1 + e_3^2)}{(1-s)^2} b_{1i} - \frac{4(c_1 - c_3 + 2e_1^2 - e_1 e_3)}{(1-s)^2} (b_{1i} - s b_{2i}) + \frac{4e_1 e_3 s}{(1-s)^2} b_{3i} + \frac{8e_1^2 s(1-s + s \ln s)}{(1-s)^3} b_{3i}$$

$$\begin{aligned}
C_{2i} &= -\frac{2c}{i\pi}, \quad D_{2i} = \frac{2c \cos i\pi}{i\pi}, \quad C_{3i} = -\frac{2}{i\pi}, \quad D_{3i} = \frac{2 \cos i\pi}{i\pi} \\
a_{1ij} &= \int_s^1 \frac{2}{\lambda} \sin \frac{\lambda-s}{1-s} i\pi \cos \frac{\lambda-s}{1-s} j\pi d\lambda, \quad a_{2ij} = \int_s^1 \frac{2}{\lambda^2} \sin \frac{\lambda-s}{1-s} i\pi \sin \frac{\lambda-s}{1-s} j\pi d\lambda \\
b_{1i} &= \int_s^1 \frac{1}{\lambda} \sin \frac{\lambda-s}{1-s} i\pi d\lambda, \quad b_{2i} = \int_s^1 \frac{1}{\lambda^2} \sin \frac{\lambda-s}{1-s} i\pi d\lambda, \quad b_{3i} = \int_s^1 \frac{1}{\lambda^3} \sin \frac{\lambda-s}{1-s} i\pi d\lambda
\end{aligned} \tag{31}$$

Eq. (29) represents a multi-degree-of-freedom control system subjected to stochastic excitations. This system has asymmetric stiffness matrix due to the boundary excitations and the electrical and mechanical coupling. Therefore, the conventional modal control method for symmetric systems is not usable to the asymmetric system. The radial stress can be derived correspondingly from Eq. (27), for instance, the boundary stress at the inner radius as

$$\begin{aligned}
\sigma_r(s, \tau) &= \frac{\pi(1+e_3^2)}{1-s} \sum_{j=1}^n j q_j - \frac{2e_1 e_3}{s(1-s)} \sum_{j=1}^n b_{1j} q_j + \left[\frac{2(c_3 + e_1 e_3)}{s} - \frac{s-(1-s)e_3^2}{s(1-s)} \right. \\
&+ \left. \frac{2e_1 e_3}{s(1-s)^2} (1-s + \ln s) \right] \xi_a + \left[\frac{s-(1-s)e_3^2}{s(1-s)} - \frac{2e_1 e_3}{s(1-s)^2} (1-s + s \ln s) \right] \xi_b \\
&- \frac{e_3}{s(1-s)} (U_a - U_b)
\end{aligned} \tag{32}$$

Based on the boundary stress expression as well as stress rate, the performance index Eq. (19) for control is converted generally into

$$J = E \left[\int_{\tau_0}^{\tau_f} L_c(\mathbf{Q}, \dot{\mathbf{Q}}, U, \tau) d\tau + \Psi(\mathbf{Q}(\tau_f), \dot{\mathbf{Q}}(\tau_f)) \right] \tag{33}$$

where L_c is a continuous differentiable function quadratic in system state $(\mathbf{Q}, \dot{\mathbf{Q}})$ and control U , Ψ is the terminal cost. The stochastic optimal control problem [Eqs. (13)-(19)] for the piezoelectric shell has been converted into that for the multi-degree-of-freedom system described by Eqs. (29) and (33).

4. Optimal control law

Rewrite Eq. (29) further in the following state equation

$$\dot{\mathbf{Z}} = \mathbf{A}\mathbf{Z} + \mathbf{F}_t \mathbf{W}(t) + \mathbf{B}_t U \tag{34}$$

where system state vector \mathbf{Z} , coefficient matrix \mathbf{A} , excitation amplitude vector \mathbf{F}_t and control coefficient vector \mathbf{B}_t are

$$\mathbf{Z} = \begin{Bmatrix} \mathbf{Q} \\ \dot{\mathbf{Q}} \end{Bmatrix}, \quad \mathbf{A} = \begin{bmatrix} 0 & \mathbf{I} \\ -\mathbf{K} & -\mathbf{C} \end{bmatrix}, \quad \mathbf{F}_t = \begin{bmatrix} 0 \\ \mathbf{F}_p \end{bmatrix}, \quad \mathbf{B}_t = \begin{Bmatrix} 0 \\ \mathbf{B} \end{Bmatrix}, \quad \mathbf{F}_p \mathbf{W}(\tau) = \mathbf{F}(\tau) \tag{35}$$

The performance index Eq. (33) is reduced to

$$J = E \left[\int_{\tau_0}^{\tau_f} (\mathbf{Z}^T \mathbf{S} \mathbf{Z} + R^2 U^2) d\tau + \Psi(\mathbf{Z}(\tau_f)) \right] \quad (36)$$

where \mathbf{S} is a positive semi-definite symmetric constant matrix and R is a constant. It is assumed that the control system Eq. (34) is completely observed. For the stochastic excitation \mathbf{W} represented as filtering white noises, applying the stochastic dynamical programming principle (Stengel 1986) to system Eq. (34) and index Eq. (36) yields the Hamilton-Jacobi-Bellman equation as follows

$$\frac{\partial V}{\partial \tau} + \min_U \{ \mathbf{Z}^T \mathbf{S} \mathbf{Z} + R^2 U^2 + (\mathbf{A} \mathbf{Z} + \mathbf{B}_i U)^T \frac{\partial V}{\partial \mathbf{Z}} + \frac{1}{2} \text{tr} [E(\mathbf{W}^T \mathbf{F}_i^T \frac{\partial^2 V}{\partial \mathbf{Z}^2} \mathbf{F}_i \mathbf{W})] \} = 0 \quad (37)$$

where V is the value function and $\text{tr}[\cdot]$ denotes the trace operation. By minimizing the left side of Eq. (37), the optimal control law obtained is

$$U^* = -\frac{1}{2R^2} \mathbf{B}_i^T \frac{\partial V}{\partial \mathbf{Z}} \quad (38)$$

Treat the optimal control of system Eq. (34) with index Eq. (36) as an optimal regulation problem. Then the stationary value function and optimal control solutions to Eq. (37) are given by

$$V = \mathbf{Z}^T \mathbf{P} \mathbf{Z}, \quad U^* = -\frac{1}{R^2} \mathbf{B}_i^T \mathbf{P} \mathbf{Z} \quad (39a,b)$$

where symmetric constant matrix \mathbf{P} is determined by the following Riccati equation

$$\mathbf{P} \mathbf{B}_i \mathbf{B}_i^T \mathbf{P} - R^2 (\mathbf{A}^T \mathbf{P} + \mathbf{P} \mathbf{A}) - R^2 \mathbf{S} = 0 \quad (40)$$

For controlling the boundary stresses of the piezoelectric shell, matrix \mathbf{S} as well as \mathbf{P} can be expressed by sub-matrices

$$\mathbf{S} = \begin{bmatrix} \mathbf{S}_1 & 0 \\ 0 & \mathbf{S}_3 \end{bmatrix}, \quad \mathbf{P} = \begin{bmatrix} \mathbf{P}_1 & \mathbf{P}_2^T \\ \mathbf{P}_2 & \mathbf{P}_3 \end{bmatrix} \quad (41a,b)$$

The optimal control of electric potential Eqs. (39(b)) and (40) are reduced respectively to

$$U^* = -\frac{1}{R^2} \mathbf{B}^T (\mathbf{P}_2 \mathbf{Q} + \mathbf{P}_3 \dot{\mathbf{Q}}) \quad (42)$$

$$\mathbf{P}_2^T \mathbf{B} \mathbf{B}^T \mathbf{P}_2 + R^2 (\mathbf{K}^T \mathbf{P}_2 + \mathbf{P}_2^T \mathbf{K}) - R^2 \mathbf{S}_1 = 0 \quad (43a)$$

$$\mathbf{P}_3 \mathbf{B} \mathbf{B}^T \mathbf{P}_3 + R^2 (\mathbf{C} \mathbf{P}_3 + \mathbf{P}_3 \mathbf{C}) - R^2 (\mathbf{P}_2 + \mathbf{P}_2^T + \mathbf{S}_3) = 0 \quad (43b)$$

Sub-matrices \mathbf{P}_2 and \mathbf{P}_3 are obtained by solving Eqs. (43(a) and (b)). The optimal electric potential control input U^* is then determined by substituting \mathbf{P}_2 and \mathbf{P}_3 with system state into Eq. (42).

5. Stochastic response estimation

Substituting the optimal control Eq. (42) into Eq. (29) yields the controlled system equation

$$\ddot{\mathbf{Q}} + (\mathbf{C} + \frac{1}{R^2} \mathbf{B} \mathbf{B}^T \mathbf{P}_3) \dot{\mathbf{Q}} + (\mathbf{K} + \frac{1}{R^2} \mathbf{B} \mathbf{B}^T \mathbf{P}_2) \mathbf{Q} = \mathbf{F}(\tau) \quad (44)$$

The instantaneous responses of the controlled piezoelectric shell subjected to stochastic excitations can be calculated rigorously by using Eqs. (44), (28), (24), (27) and (20). The response statistics of the controlled asymmetric linear multi-degree-of-freedom system Eq. (44) can be estimated by using the relationship between the correlation function in time domain and the power spectral density in frequency domain. The frequency-response function matrix of the system Eq. (44) is

$$\mathbf{H}(j\omega) = [\mathbf{K} + \frac{1}{R^2} \mathbf{B}\mathbf{B}^T \mathbf{P}_2 + j\omega(\mathbf{C} + \frac{1}{R^2} \mathbf{B}\mathbf{B}^T \mathbf{P}_3) - \omega^2 \mathbf{I}]^{-1} \quad (45)$$

where \mathbf{I} is the identity matrix, ω is a frequency and $j = \sqrt{-1}$. Then the power spectral density matrix of the system response is correspondingly

$$\mathbf{S}_Q(\omega) = \mathbf{H}(j\omega)\mathbf{S}_F(\omega)\mathbf{H}^T(j\omega) \quad (46)$$

where $\mathbf{S}_F(\omega)$ is the spectral density matrix of the system excitation $\mathbf{F}(\tau)$, and the superscript “ T ” denotes the conjugate and transpose operation. The spectral density $\mathbf{S}_F(\omega)$ can be calculated by using Eq. (30(b)). For independent stochastic boundary perturbation excitations $\xi_a(\tau)$ and $\xi_b(\tau)$ with respectively spectral densities $S_{\xi_a}(\omega)$ and $S_{\xi_b}(\omega)$, the element in the spectral density matrix $\mathbf{S}_F(\omega)$ is

$$\begin{aligned} [\mathbf{S}_F(\omega)]_{ik} = & [C_{1i}C_{1k} + (C_{2i}C_{2k} - C_{1i}C_{3k} - C_{3i}C_{1k})\omega^2 + C_{3i}C_{3k}\omega^4 + (C_{2i}C_{1k} - C_{1i}C_{2k})j\omega \\ & + (C_{3i}C_{2k} - C_{2i}C_{3k})j\omega^3]S_{\xi_a}(\omega) + [D_{1i}D_{1k} + (D_{2i}D_{2k} - D_{1i}D_{3k} - D_{3i}D_{1k})\omega^2 \\ & + D_{3i}D_{3k}\omega^4 + (D_{2i}D_{1k} - D_{1i}D_{2k})j\omega + (D_{3i}D_{2k} - D_{2i}D_{3k})j\omega^3]S_{\xi_b}(\omega) \end{aligned} \quad (47)$$

The natural frequencies of the system Eq. (44) or the piezoelectric shell can be obtained by the peak-value characteristics of the frequency-response function $\mathbf{H}(j\omega)$, and the response spectra are determined by spectral density matrix $\mathbf{S}_Q(\omega)$. The correlation function matrices of the system response (\mathbf{Q} , $\dot{\mathbf{Q}}$) can be expressed as

$$\mathbf{R}_Q(0) = \int_{-\infty}^{\infty} \mathbf{S}_Q(\omega)d\omega, \quad \mathbf{R}_{\dot{Q}}(0) = \int_{-\infty}^{\infty} \omega^2 \mathbf{S}_Q(\omega)d\omega, \quad \mathbf{R}_{Q\dot{Q}}(0) = \int_{-\infty}^{\infty} -j\omega \mathbf{S}_Q(\omega)d\omega \quad (48a,b,c)$$

The mean-square response such as $E[q_i^2]$ of the controlled multi-degree-of-freedom system Eq. (44) is determined by the diagonal elements of the correlation function matrix $\mathbf{R}_Q(0)$. The mean-square optimal electric potential control is obtained from Eq. (42) as

$$E[U^{*2}] = \frac{1}{R^4} \mathbf{B}^T (\mathbf{P}_2 \mathbf{R}_Q \mathbf{P}_2^T + \mathbf{P}_3 \mathbf{R}_{\dot{Q}} \mathbf{P}_3 + \mathbf{P}_2 \mathbf{R}_{Q\dot{Q}} \mathbf{P}_3 + \mathbf{P}_3 \mathbf{R}_{Q\dot{Q}}^T \mathbf{P}_2^T) \mathbf{B} \quad (49)$$

Further, the displacement, stress and electric potential expressions of the controlled piezoelectric shell are obtained by substituting Eq. (28) respectively into Eqs. (24), (27) and (20) as follows

$$v(\lambda, \tau) = \mathbf{L}(\lambda)^T \mathbf{Q} + E_5(\lambda) \xi_a + E_6(\lambda) \xi_b \quad (50)$$

$$\sigma_r(\lambda, \tau) = \mathbf{N}(\lambda)^T \mathbf{Q} + E_3(\lambda) \xi_a + E_4(\lambda) \xi_b + R_s(\lambda) U^* \quad (51)$$

$$\phi_r(\lambda, \tau) = \mathbf{M}(\lambda)^T \mathbf{Q} + E_1(\lambda) \xi_a + E_2(\lambda) \xi_b + R_e(\lambda) U^* \quad (52)$$

where the electric potential ϕ_r is relative to that at the outer radius

$$\begin{aligned}
 \mathbf{L} &= [L_1, L_2, \dots, L_n]^T, \quad \mathbf{N} = [N_1, N_2, \dots, N_n]^T, \quad \mathbf{M} = [M_1, M_2, \dots, M_n]^T \\
 L_i &= \sin \frac{\lambda-s}{1-s} i\pi, \quad M_i = 2e_1 b'_{1i} - \frac{2e_1(\lambda-s)}{\lambda(1-s)} b_{1i} + e_3 \sin \frac{\lambda-s}{1-s} i\pi \\
 N_i &= \frac{2(c_3 + e_1 e_3)}{\lambda} \sin \frac{\lambda-s}{1-s} i\pi + \frac{i\pi(1+e_3^2)}{1-s} \cos \frac{\lambda-s}{1-s} i\pi - \frac{2e_1 e_3 s}{\lambda^2(1-s)} b_{1i} \\
 b'_{1i}(\lambda) &= \int_s^1 \frac{1}{x} \sin \frac{x-s}{1-s} i\pi dx, \quad E_5 = -\frac{\lambda-1}{1-s}, \quad E_6 = \frac{\lambda-s}{1-s} \\
 E_3 &= 2(c_3 + e_1 e_3) \frac{1-\lambda}{\lambda(1-s)} - \frac{1+e_3^2}{1-s} + \frac{2e_1 e_3 s}{\lambda^2(1-s)^2} (1-s + \ln s) + \frac{e_3^2 s}{\lambda^2(1-s)} \\
 E_4 &= 2(c_3 + e_1 e_3) \frac{\lambda-s}{\lambda(1-s)} + \frac{1+e_3^2}{1-s} - \frac{2e_1 e_3 s}{\lambda^2(1-s)^2} (1-s + s \ln s) - \frac{e_3^2 s}{\lambda^2(1-s)} \\
 E_1 &= \frac{2e_1(\ln \lambda - \lambda - \ln s + s)}{1-s} + \frac{e_3(1-\lambda)(\lambda-s)}{\lambda(1-s)} + \frac{2e_1(\lambda-s)(1-s + \ln s)}{\lambda(1-s)^2} \\
 E_2 &= \frac{2e_1(\lambda-s \ln \lambda - s + s \ln s)}{1-s} - \frac{e_3(1-\lambda)(\lambda-s)}{\lambda(1-s)} + \frac{2e_1(s-\lambda)(1-s + s \ln s)}{\lambda(1-s)^2} \\
 R_s &= -\frac{e_3 s}{\lambda^2(1-s)}, \quad R_e = \frac{s(1-\lambda)}{\lambda(1-s)}
 \end{aligned} \tag{53}$$

By using Eqs. (50)-(52), (48) and (42), the response statistics of the controlled piezoelectric shell subjected to stochastic boundary perturbations can be calculated rigorously. The mean-square displacement, stress and electric potential of the shell are obtained as

$$\begin{aligned}
 E[v^2](\lambda) &= \mathbf{L}^T \mathbf{R}_Q \mathbf{L} + \mathbf{L}^T (E_5 E[\mathbf{Q}\xi_a] + E_6 E[\mathbf{Q}\xi_b]) + E_5^2 E[\xi_a^2] \\
 &\quad + (E_5 E[\xi_a \mathbf{Q}^T] + E_6 E[\xi_b \mathbf{Q}^T]) \mathbf{L} + E_6^2 E[\xi_b^2]
 \end{aligned} \tag{54}$$

$$\begin{aligned}
 E[\sigma_r^2](\lambda) &= \mathbf{N}^T \mathbf{R}_Q \mathbf{N} + \mathbf{N}^T (E_3 E[\mathbf{Q}\xi_a] + E_4 E[\mathbf{Q}\xi_b] + R_s E[\mathbf{Q}U^*]) \\
 &\quad + (E_3 E[\xi_a \mathbf{Q}^T] + E_4 E[\xi_b \mathbf{Q}^T] + R_s E[U^* \mathbf{Q}^T]) \mathbf{N} + E_3^2 E[\xi_a^2] + E_4^2 E[\xi_b^2] \\
 &\quad + E_3 R_s (E[\xi_a U^*] + E[U^* \xi_a]) + E_4 R_s (E[\xi_b U^*] + E[U^* \xi_b]) + R_s^2 E[U^{*2}]
 \end{aligned} \tag{55}$$

$$\begin{aligned}
 E[\phi_r^2](\lambda) &= \mathbf{M}^T \mathbf{R}_Q \mathbf{M} + \mathbf{M}^T (E_1 E[\mathbf{Q}\xi_a] + E_2 E[\mathbf{Q}\xi_b] + R_e E[\mathbf{Q}U^*]) \\
 &\quad + (E_1 E[\xi_a \mathbf{Q}^T] + E_2 E[\xi_b \mathbf{Q}^T] + R_e E[U^* \mathbf{Q}^T]) \mathbf{M} + E_1^2 E[\xi_a^2] + E_2^2 E[\xi_b^2] \\
 &\quad + E_1 R_e (E[\xi_a U^*] + E[U^* \xi_a]) + E_2 R_e (E[\xi_b U^*] + E[U^* \xi_b]) + R_e^2 E[U^{*2}]
 \end{aligned} \tag{56}$$

where the cross-correlation function vectors of the system response (\mathbf{Q}) and the boundary perturbations (ξ_a and ξ_b) and the optimal control (U^*), and the mean-square boundary perturbations are

$$\begin{aligned}
E[\mathbf{Q}\xi_a] &= \int_{-\infty}^{\infty} \mathbf{S}_{Q\xi_a}(\omega)d\omega, \quad E[\xi_a\mathbf{Q}^T] = E[\mathbf{Q}\xi_a]^T, \quad E[\mathbf{Q}\xi_b] = \int_{-\infty}^{\infty} \mathbf{S}_{Q\xi_b}(\omega)d\omega \\
E[\xi_b\mathbf{Q}^T] &= E[\mathbf{Q}\xi_b]^T, \quad E[\xi_a^2] = \int_{-\infty}^{\infty} S_{\xi_a}(\omega)d\omega, \quad E[\xi_b^2] = \int_{-\infty}^{\infty} S_{\xi_b}(\omega)d\omega \\
E[U^*\mathbf{Q}^T] &= -\frac{1}{R^2}\mathbf{B}^T(\mathbf{P}_2\mathbf{R}_Q + \mathbf{P}_3\mathbf{R}_{Q\dot{Q}}), \quad E[\mathbf{Q}U^*] = E[U^*\mathbf{Q}^T]^T \\
E[U^*\xi_a] &= -\frac{1}{R^2}\mathbf{B}^T(\mathbf{P}_2E[\mathbf{Q}\xi_a] + \mathbf{P}_3E[\dot{\mathbf{Q}}\xi_a]), \quad E[\xi_aU^*] = E[U^*\xi_a]^T \\
E[U^*\xi_b] &= -\frac{1}{R^2}\mathbf{B}^T(\mathbf{P}_2E[\mathbf{Q}\xi_b] + \mathbf{P}_3E[\dot{\mathbf{Q}}\xi_b]), \quad E[\xi_bU^*] = E[U^*\xi_b]^T \\
E[\dot{\mathbf{Q}}\xi_a] &= \int_{-\infty}^{\infty} j\omega\mathbf{S}_{Q\xi_a}(\omega)d\omega, \quad E[\dot{\mathbf{Q}}\xi_b] = \int_{-\infty}^{\infty} j\omega\mathbf{S}_{Q\xi_b}(\omega)d\omega
\end{aligned} \tag{57}$$

in which the cross power spectral density vectors

$$\mathbf{S}_{Q\xi_a}(\omega) = \mathbf{H}(j\omega)\mathbf{S}_{F\xi_a}(\omega), \quad \mathbf{S}_{Q\xi_b}(\omega) = \mathbf{H}(j\omega)\mathbf{S}_{F\xi_b}(\omega) \tag{58a,b}$$

with elements

$$[\mathbf{S}_{F\xi_a}]_i = (C_{1i} + j\omega C_{2i} - \omega^2 C_{3i})S_{\xi_a}(\omega), \quad [\mathbf{S}_{F\xi_b}]_i = (D_{1i} + j\omega D_{2i} - \omega^2 D_{3i})S_{\xi_b}(\omega) \tag{59a,b}$$

Eqs. (54)-(56) represent the mean-square displacement, stress and electric potential as functions of dimensionless radial coordinate λ , which can be used for exploring the response characteristics and the control effectiveness of the controlled piezoelectric shell subjected to stochastic boundary displacement perturbations. The stochastic response of the uncontrolled piezoelectric shell subjected to boundary displacement perturbations can be estimated by using the above equations with zero control.

6. Numerical results

Consider the stochastic optimal control of the PZT-4 piezoelectric spherically symmetric shell subjected to stochastic boundary displacement perturbations. The basic structure, excitation and control parameters (Ying *et al.* 2009, Berlincourt *et al.* 1964) are $c_{11}=139.0$ GPa, $c_{12}=77.8$ GPa, $c_{13}=74.3$ GPa, $c_{33}=115.0$ GPa, $e_{31}=-5.2$ C/m², $e_{33}=15.1$ C/m², $e_{33}=5.62 \times 10^{-9}$ C²/N·m², $s=a/b=0.5$, $c=0.5$; $\omega_0=7.5$, $s_0=5 \times 10^{-11}$, $\eta=0.05$, $S_{\xi_a}(\omega)=0$, $U_b=0$ (or $\phi_r=\phi$); $\mathbf{S}_1=\text{diag} [10, 10, 2 \times 10^6, 2 \times 10^5, 0, \dots]$ and $\mathbf{S}_2=0$ except the otherwise pointed. The boundary perturbation spectral density at the outer radius and the weighting constant in performance index for controlling boundary stresses are respectively

$$S_{\xi_b}(\omega) = \frac{S_0}{(\omega_0^2 - \omega^2) + (2\eta\omega)^2}, \quad R = \frac{-e_3}{s(1-s)} \tag{60a,b}$$

Numerical results on the frequency-response functions, root-mean-square stresses, displacements electric potentials and optimal controls have been obtained and shown in Figs. 1-15.

Fig. 1 shows the frequency-response functions $H_{11}(\omega)$, $H_{22}(\omega)$, $H_{33}(\omega)$ and $H_{44}(\omega)$ in matrix $\mathbf{H}(\omega)$

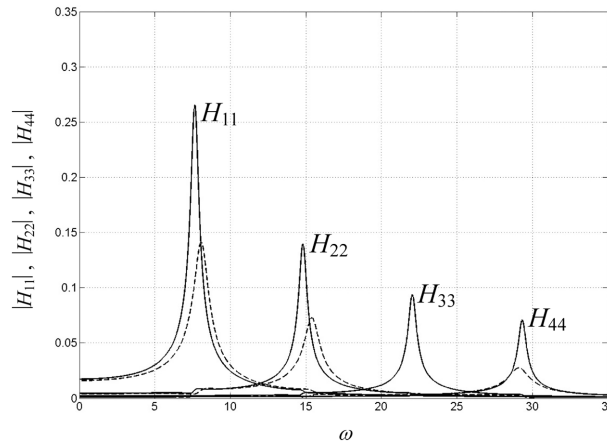


Fig. 1 Frequency-response functions $H_{11}(\omega)$, $H_{22}(\omega)$, $H_{33}(\omega)$ and $H_{44}(\omega)$ (Uncontrolled - solid line; Controlled - dashed line)

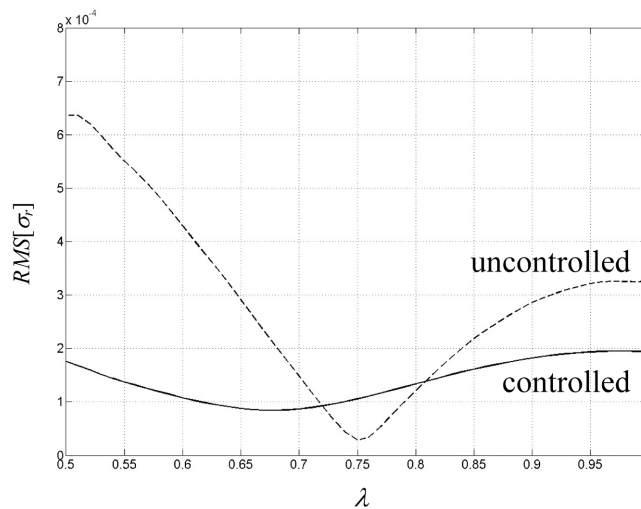


Fig. 2 Root-mean-square (RMS) radial stress (σ_r) versus dimensionless radial coordinate λ

varying with frequency ω for the controlled and uncontrolled piezoelectric shells. It can be seen that the first four dimensionless natural frequencies of the uncontrolled shell are $\omega_1=7.64$, $\omega_2=14.80$, $\omega_3=22.04$ and $\omega_4=29.32$. Figs. 2-4 illustrate the root-mean-square radial stress (σ_r), radial displacement (v) and electric potential (ϕ) varying with the dimensionless radial coordinate (λ) for the controlled and uncontrolled piezoelectric shells, respectively. The controlled root-mean-square stress and displacement change much slowly along the shell radius than the uncontrolled ones. The relative reductions of the controlled root-mean-square stress at the inner radius and displacement at $\lambda=0.75$ come to 72% and 58%, respectively, under the root-mean-square optimal control of electric potential at the inner radius $U^*=1.2 \times 10^{-4}$. The samples of boundary displacement perturbation (ξ_b), uncontrolled and controlled stress (σ_r) at the inner radius and electric potential control (U^*) are shown in Figs. 5-7.

Figs. 8-12 illustrate the root-mean-square radial stress (σ_r), radial displacement (v) and electric potential (ϕ) of the controlled and uncontrolled piezoelectric shells varying with the dimensionless

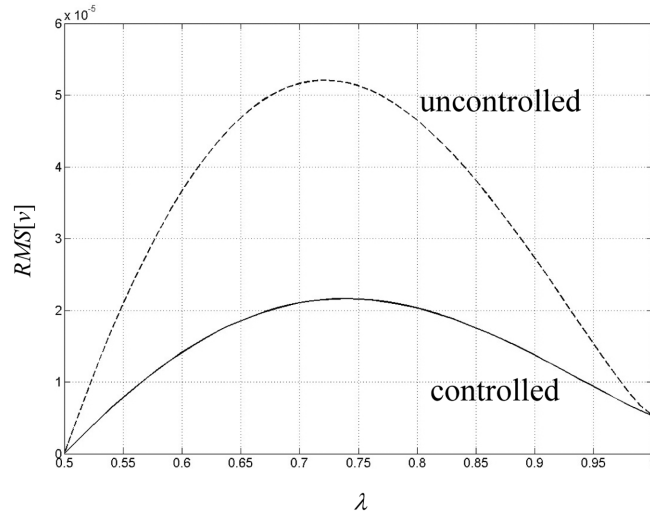


Fig. 3 Root-mean-square (RMS) radial displacement (v) versus dimensionless radial coordinate λ

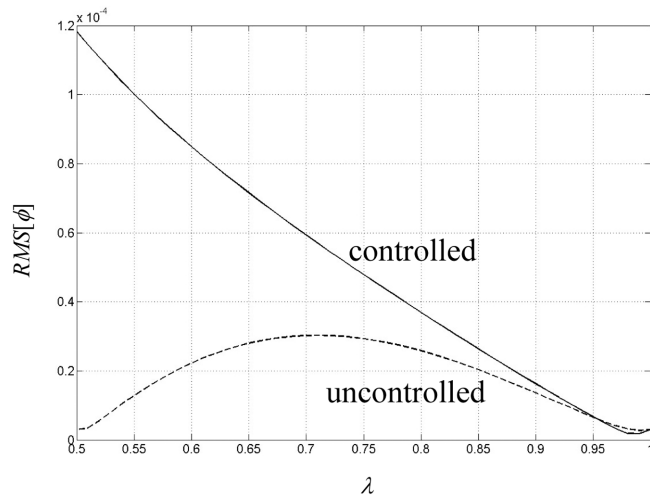


Fig. 4 Root-mean-square (RMS) electric potential (ϕ) versus dimensionless radial coordinate λ

radial coordinate (λ) for different elastic, piezoelectric and dielectric constants, respectively. The root-mean-square stress and displacement increase as the elastic constants c_{11} decreases or c_{33} increases, as shown in Figs. 8 and 9. The effects of the elastic constants on the controlled root-mean-square stress and displacement are less than uncontrolled ones. Then the control effectiveness such as the relative reduction of the controlled root-mean-square stress at the inner radius is heightened correspondingly. The dependence of the root-mean-square stress and displacement upon the piezoelectric constant e_{33} and dielectric constant ϵ_{33} similar to the elastic constants c_{11} and c_{33} can be observed by Figs. 11 and 12. However, as shown in Fig. 10, the piezoelectric constant e_{31} has more effects on the controlled root-mean-square stress and displacement than uncontrolled ones.

Figs. 13 and 14 illustrate the control effectiveness or the relative reduction of the controlled root-mean-square radial stress (σ_r) at the inner radius and the root-mean-square electric potential control

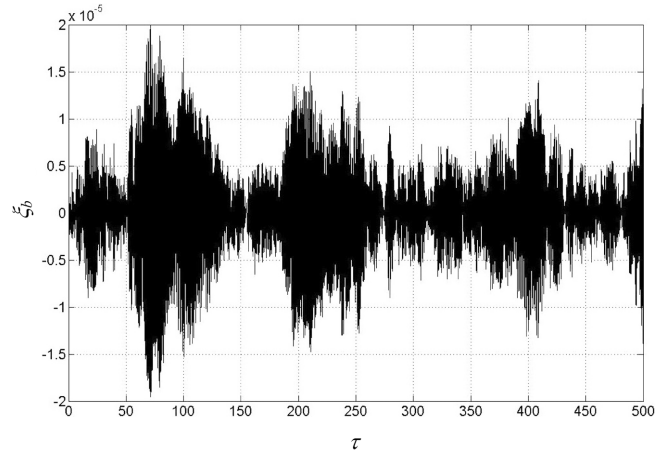


Fig. 5 A sample of radial displacement at the outer radius or boundary perturbation (ξ_b)

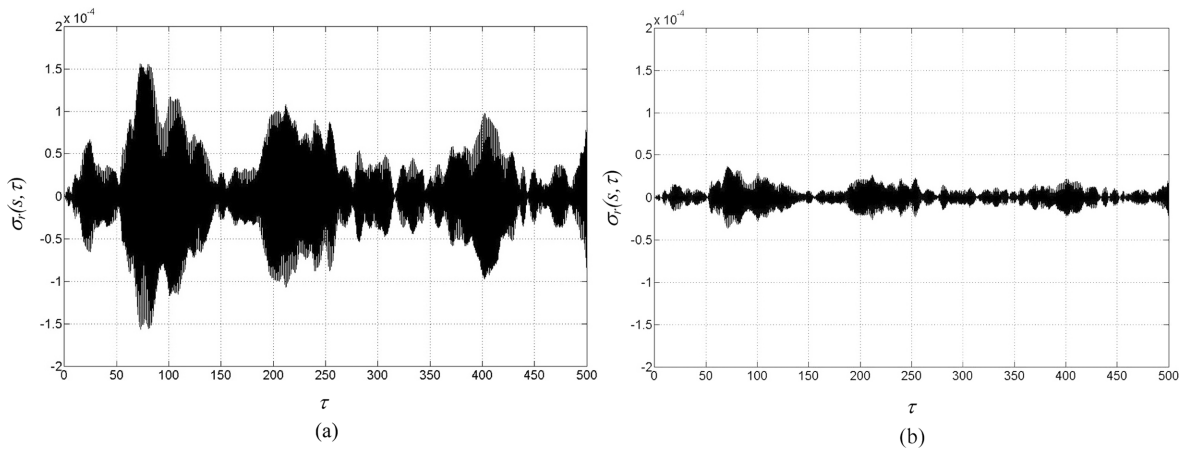


Fig. 6 Samples of radial stress (σ_r) at the inner radius ((a) Uncontrolled and (b) controlled)

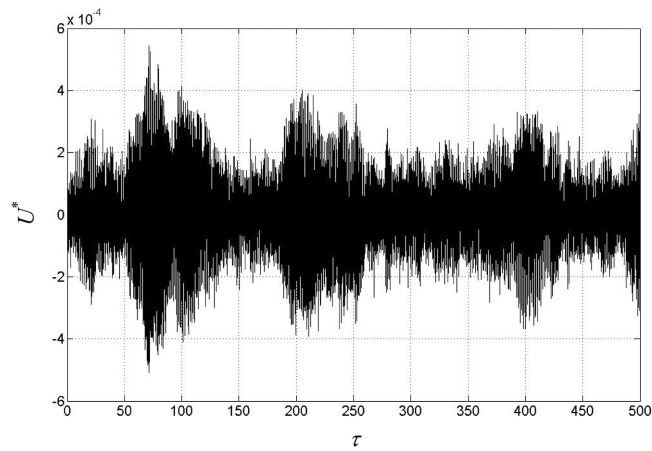


Fig. 7 A sample of electric potential at the inner radius or control input (U^*)

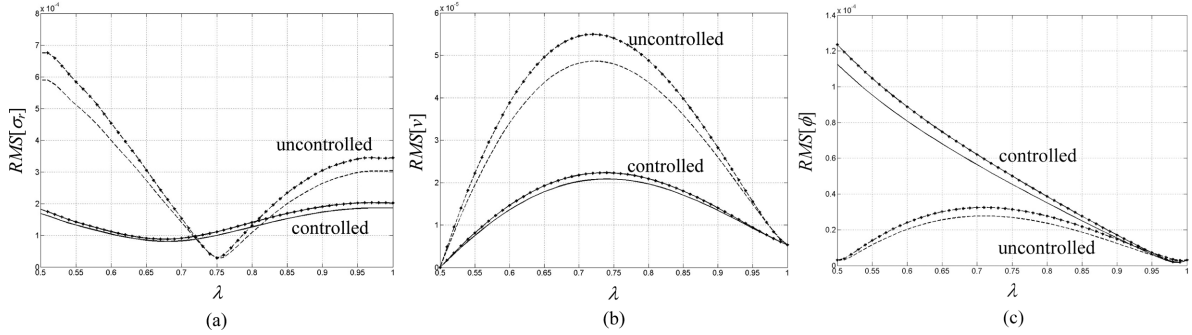


Fig. 8 Root-mean-square (RMS) radial stress, radial displacement and electric potential versus dimensionless radial coordinate λ for different elastic constant c_{11} ($c_{11}=120$ GPa - line with asterisk; $c_{11}=160$ GPa - line without asterisk). (a) radial stress σ_r , (b) radial displacement v and (c) electric potential ϕ

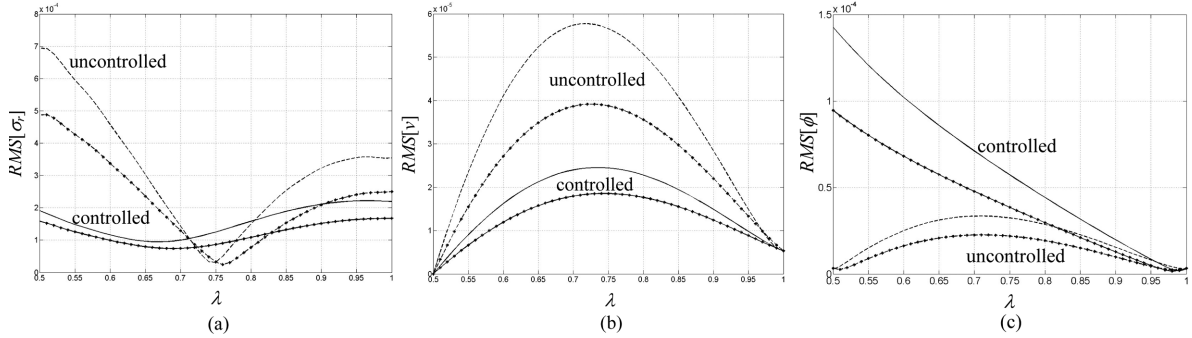


Fig. 9 Root-mean-square (RMS) radial stress, radial displacement and electric potential versus dimensionless radial coordinate λ for different elastic constant c_{33} ($c_{33}=100$ GPa - line with asterisk; $c_{33}=130$ GPa - line without asterisk). (a) radial stress σ_r , (b) radial displacement v and (c) electric potential ϕ

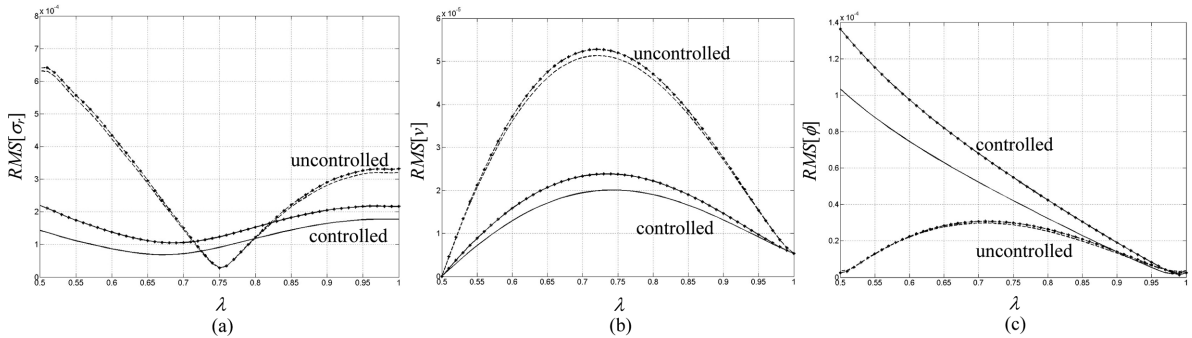


Fig. 10 Root-mean-square (RMS) radial stress, radial displacement and electric potential versus dimensionless radial coordinate λ for different piezoelectric constant e_{31} ($e_{31}=-4.2$ C/m² - line with asterisk; $e_{31}=-6.2$ C/m² - line without asterisk). (a) radial stress σ_r , (b) radial displacement v and (c) electric potential ϕ

input (U^*) varying with the stochastic boundary perturbation intensity s_0 and dominant frequency ω_0 , respectively. As the perturbation intensity s_0 rises, the root-mean-square electric potential control is enhanced correspondingly so that the relative reduction of the controlled root-mean-square stress is held, as shown in Figs. 13(a) and (b). The dominant perturbation frequency ω_0 has obvious

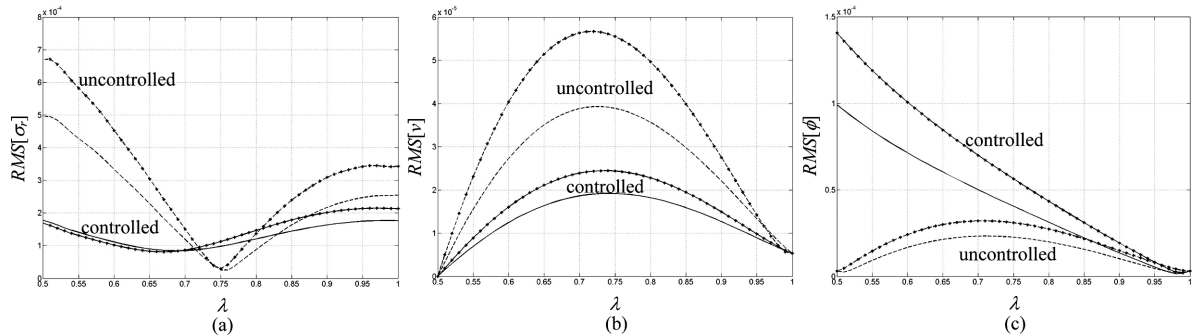


Fig. 11 Root-mean-square (RMS) radial stress, radial displacement and electric potential versus dimensionless radial coordinate λ for different piezoelectric constant e_{33} ($e_{33}=13.6 \text{ C/m}^2$ - line with asterisk; $e_{33}=16.6 \text{ C/m}^2$ - line without asterisk). (a) radial stress σ_r , (b) radial displacement v and (c) electric potential ϕ

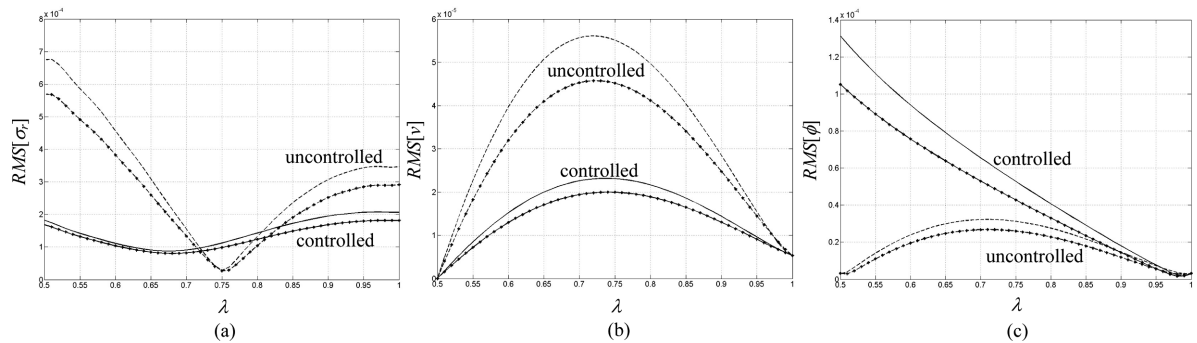


Fig. 12 Root-mean-square (RMS) radial stress, radial displacement and electric potential versus dimensionless radial coordinate λ for different dielectric constant ϵ_{33} ($\epsilon_{33}=5.12 \times 10^{-9} \text{ C}^2/\text{Nm}^2$ - line with asterisk; $\epsilon_{33}=6.12 \times 10^{-9} \text{ C}^2/\text{Nm}^2$ - line without asterisk). (a) radial stress σ_r , (b) radial displacement v and (c) electric potential ϕ

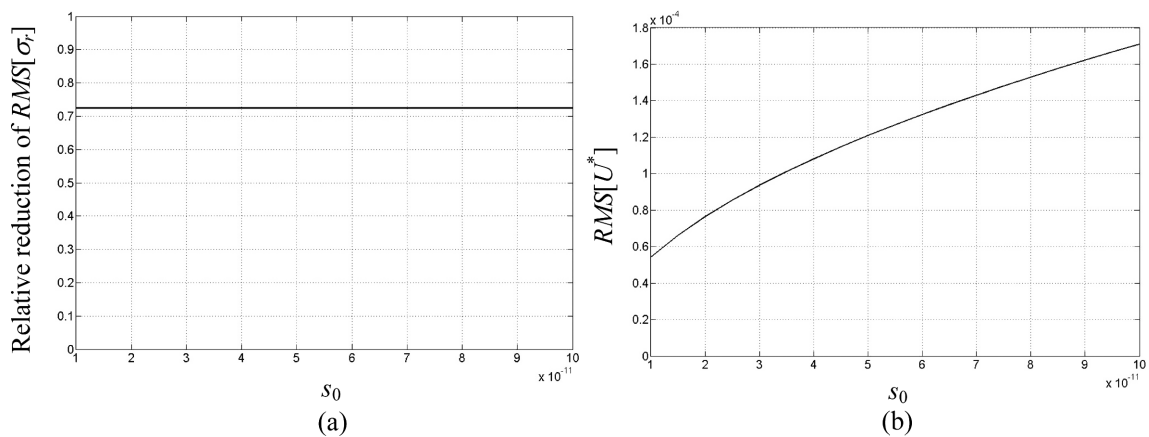


Fig. 13 Control effectiveness and control input versus stochastic perturbation intensity s_0 . (a) relative reduction of the controlled root-mean-square boundary stress σ_r and (b) root-mean-square electric potential control input U^*

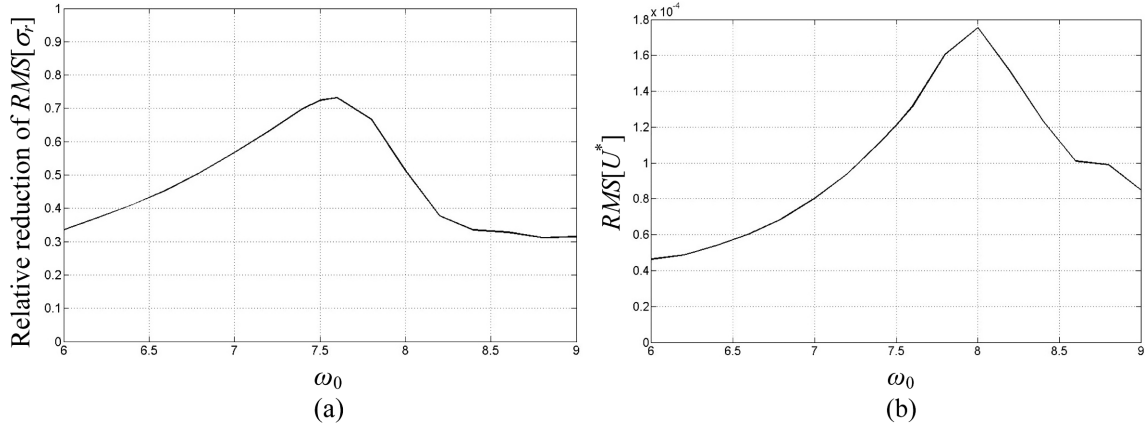


Fig. 14 Control effectiveness and control input versus dominant perturbation frequency ω_0 . (a) relative reduction of the controlled root-mean-square boundary stress σ_r and (b) root-mean-square electric potential control input U^*

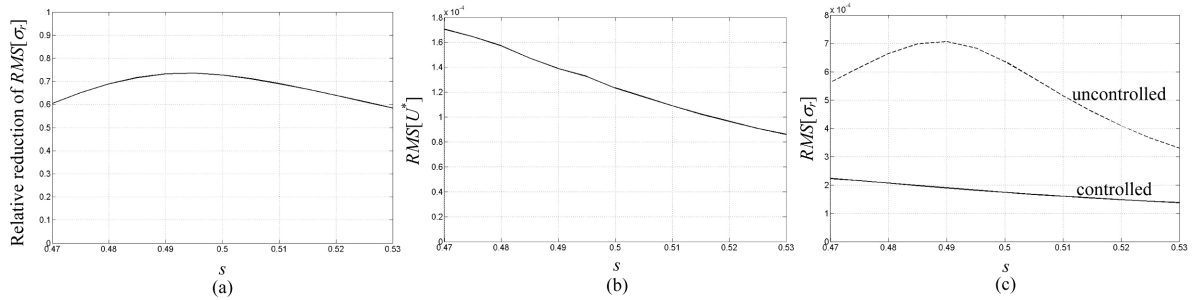


Fig. 15 Control effectiveness and control input versus ratio s of inner to outer radii. (a) relative reduction of the controlled root-mean-square boundary stress σ_r , (b) root-mean-square electric potential control input U^* and (c) comparison between controlled and uncontrolled root-mean-square boundary stresses

influence on the optimal control (electric potential) and the control effectiveness (relative reduction of the controlled root-mean-square stress), as shown in Figs. 14(a) and (b). There exists an optimum control design to achieve the optimal control effectiveness for certain dominant perturbation frequency. Figs. 15(a) and (b) show respectively the control effectiveness and corresponding optimal control varying with the ratio s of inner radius to outer radius. The root-mean-square electric potential control input is diminished with the increase of the ratio s due to the decreased uncontrolled root-mean-square boundary stress (Fig. 15(c)). The numerical results above indicate that the root-mean-square boundary radial stress of the piezoelectric shell subjected to stochastic boundary displacement perturbations can be optimally controlled to the relative reduction of 70% by the electric potential control input according to the proposed stochastic optimal control.

7. Conclusions

The stochastic optimal control for piezoelectric spherically symmetric shells subjected to stochastic boundary perturbations has been proposed and analyzed by the electric potential integral, displacement

transformation, Galerkin method, stochastic dynamical programming and stochastic response estimation. The proposed optimal control is applicable to the spherical shells with arbitrary thickness under various non-white stochastic excitations at inner and/or outer surfaces. The stochastic optimal control problem of the piezoelectric shell structure has been converted into that of the multi-degree-of-freedom system, and the optimal control law for electric potential has been determined. The root-mean-square stresses, displacements and electric potentials of the controlled and uncontrolled shells as well as the control effectiveness have been obtained, and illustrated with a great deal of numerical results on the piezoelectric shell with various structural and excitation parameters. The high relative reduction in the root-mean-square boundary stress of the piezoelectric shell subjected to stochastic boundary displacement perturbations can be achieved by the proposed optimal electric potential control.

Acknowledgements

This study was supported by the National Natural Science Foundation of China under Grant Nos. 10932009 and 11072215, the Zhejiang Provincial Natural Science Foundation of China under Grant No. Y607087 and the Scientific Research Fund of Zhejiang Provincial Education Department under Grant No. Y200907048. The authors are grateful for the supports.

References

- Adelman, N.T., Stavsky, Y. and Segal, E. (1975), "Axisymmetric vibration of radially polarized piezoelectric ceramic cylinders", *J. Sound Vib.*, **38**(2), 245-254.
- Babaev, A.E., But, L.M. and Savin, V.G. (1990), "Transient vibrations of a thin-walled cylindrical piezoelectric vibrator driven by a nonaxisymmetric electric signal in a liquid", *Int. Appl. Mech.*, **26**(12), 1167-1174.
- Balamurugan, V. and Narayanan, S. (2001), "Active vibration control of smart shells using distributed piezoelectric sensors and actuators", *Smart Mater. Struct.*, **10**(2), 173-180.
- Berg, M., Hagedorn, P. and Gutschmidt, S. (2004), "On the dynamics of piezoelectric cylindrical shells", *J. Sound Vib.*, **274**(1-2), 91-109.
- Berlincourt, D.A., Curran, D.R. and Jaffe, H. (1964), *Piezoelectric and piezomagnetic materials and their function in transducers*, Physical Acoustics: Principle and Methods, Academic Press, London.
- Borisyuk, A.I. and Kirichok, I.F. (1979), "Steady-state radial vibrations of piezoelectric spheres in compressible fluid", *Int. Appl. Mech.*, **15**(10), 936-940.
- Chen, W.Q., Ding, H.J. and Xu, R.Q. (2001), "Three dimensional free vibration analysis of a fluid-filled piezoelectric hollow sphere", *Comput. Struct.*, **79**(6), 653-663.
- Correia, I.F.P., Soares, C.M.M., Soares, C.A.M. and Herskovits, J. (2002), "Active control of axisymmetric shells with piezoelectric layers: a mixed laminated theory with a high order displacement field", *Comput. Struct.*, **80**(27-30), 2265-2275.
- Ding, H.J., Wang, H.M. and Chen, W.Q. (2003), "Transient responses in a piezoelectric spherically isotropic hollow sphere for symmetric problems", *J. Appl. Mech.*, **70**(3), 436-445.
- Ding, H.J., Wang, H.M. and Hou, P.F. (2003), "The transient responses of piezoelectric hollow cylinders for axisymmetric plane strain problems", *Int. J. Solids Struct.*, **40**(1), 105-123.
- Ding, H.J., Xu, R.Q. and Chen, W.Q. (2002), "Free vibration of transversely isotropic piezoelectric circular cylindrical panels", *Int. J. Mech. Sci.*, **44**(1), 191-206.
- Gupta, V.K., Seshu, P. and Issac, K.K. (2004), "Finite element and experimental investigation of piezoelectric actuated smart shells", *AIAA J.*, **42**(10), 2112-2123.

- Hasheminejad, S.M. and Rajabi, M. (2008), "Scattering and active acoustic control from a submerged piezoelectric-coupled orthotropic hollow cylinder", *J. Sound Vib.*, **318**(1-2), 50-73.
- Heyliger, P. and Wu, Y.C. (1999), "Electroelastic fields in layered piezoelectric spheres", *Int. J. Eng. Sci.*, **37**(2), 143-161.
- Huang, Y.M. and Tseng, H.C. (2008), "Active piezoelectric dynamic absorbers on vibration and noise reductions of the fuselage", *J. Mech.*, **24**, 69-77.
- Jin, Z.L., Yang, Y.W. and Soh, C.K. (2010), "Semi-analytical solutions for optimal distributions of sensors and actuators in smart structure vibration control", *Smart Struct. Syst.*, **6**(7), 767-792.
- Kumar, R., Mishra, B. and Jain, S. (2008), "Vibration control of smart composite laminated spherical shell using neural network", *J. Intell. Mater. Sys. Struct.*, **19**(8), 947-957.
- Li, D.S., Cheng, L. and Gosselin, C.M. (2004), "Optimal design of PZT actuators in active structural acoustic control of a cylindrical shell with a floor partition", *J. Sound Vib.*, **269**(3-5), 569-588.
- Li, H.Y., Liu, Z.X. and Lin, Q.R. (2000), "Spherical-symmetric steady-state response of piezoelectric spherical shell under external excitation", *Appl. Math. Mech. - ENGL.*, **21**(8), 947-956.
- Li, X. and Zhang, Y.F. (2008), "Feasibility study of wide-band low-profile ultrasonic sensor with flexible piezoelectric paint", *Smart Struct. Syst.*, **4**(5), 565-582.
- Loza, I.A. and Shul'ga, N.A. (1990), "Forced axisymmetric vibrations of a hollow piezoelectric sphere with an electrical method of excitation", *Int. Appl. Mech.*, **26**(9), 818-822.
- Narayanan, S. and Balamurugan, V. (2003), "Finite element modelling of piezolaminated smart structures for active vibration control with distributed sensors and actuators", *J. Sound Vib.*, **262**(3), 529-562.
- Park, S., Yun, C.B., Roh, Y. and Lee, J.J. (2005), "Health monitoring of steel structures using impedance of thickness modes at PZT patches", *Smart Struct. Syst.*, **1**(4), 339-353.
- Paul, H.S. and Venkatesan, M. (1987), "Vibration of a hollow circular cylinder of piezoelectric ceramics", *J. Acoust. Soc. Am.*, **82**, 952-956.
- Puzyrev, V. (2010), "Elastic waves in piezoceramic cylinders of sector cross-section", *Int. J. Solids Struct.*, **47**(16), 2115-2122.
- Rao, S.S. and Sunar, M. (1994), "Piezoelectricity and its use in disturbance sensing and control of flexible structures: a survey", *Appl. Mech. Rev.*, **47**(4), 113-123.
- Ray, M.C. (2003), "Optimal control of laminated shells using piezoelectric sensor and actuator layers", *AIAA J.*, **41**(6), 1151-1157.
- Roy, T. and Chakraborty, D. (2009), "Genetic algorithm based optimal control of smart composite shell structures under mechanical loading and thermal gradient", *Smart Mater. Struct.*, **18**(11), 115006.
- Rudolf, C., Martin, T. and Wauer, J. (2010), "Control of PKM machine tools using piezoelectric self-sensing actuators on basis of the functional principle of a scale with a vibrating string", *Smart Struct. Syst.*, **6**(2), 167-182.
- Saravanos, D.A. and Heyliger, P.R. (1999), "Mechanics and computational models for laminated piezoelectric beams, plates and shells", *Appl. Mech. Rev.*, **52**(10), 305-320.
- Sarma, K.V. (1980), "Torsional wave motion of a finite inhomogeneous piezoelectric cylindrical shell", *Int. J. Eng. Sci.*, **18**(3), 449-454.
- Scandrett, C. (2002), "Scattering and active acoustic control from a submerged spherical shell", *J. Acoust. Soc. Am.*, **111**(2), 893-907.
- Sheng, G.G. and Wang, X. (2009), "Active control of functionally graded laminated cylindrical shells", *Compos. Struct.*, **90**(4), 448-457.
- Shul'ga, N.A., Grigorenko, A.Y. and Loza, I.A. (1984), "Axisymmetric electroelastic waves in a hollow piezoelectric ceramic cylinder", *Int. Appl. Mech.*, **20**(1), 23-28.
- Sohn, J.W., Choi, S.B. and Lee, C.H. (2009), "Active vibration control of smart hull structure using piezoelectric composite actuators", *Smart Mater. Struct.*, **18**, 074004.
- Stengel, R.F. (1986), *Stochastic Optimal Control: Theory and Application*, John Wiley & Sons, New York.
- Tawie, R., Lee, H.K. and Park, S.H. (2010), "Non-destructive evaluation of concrete quality using PZT transducers", *Smart Struct. Syst.*, **6**(7), 851-866.
- To, C.W.S. and Chen, T. (2007), "Optimal control of random vibration in plate and shell structures with distributed piezoelectric components", *Int. J. Mech. Sci.*, **49**(12), 1389-1398.
- Trajkov, T.N., Koppe, H. and Gabbert, U. (2006), "Vibration control of a funnel-shaped shell structure with distributed piezoelectric actuators and sensors", *Smart Mater. Struct.*, **15**(4), 1119-1132.

- Tzou, H.S., Wang, D.W. and Chai, W.K. (2002), "Dynamics and distributed control of conical shells laminated with full and diagonal actuators", *J. Sound Vib.*, **256**(1), 65-79.
- Tzou, H.S. and Zhong, J.P. (1994), "A linear theory of piezoelastic shell vibrations", *J. Sound Vib.*, **175**(1), 77-88.
- Ying, Z.G, Feng, J., Ni, Y.Q. and Zhu, W.Q. (2011), "Electric potential response analysis of a piezoelectric shell under random micro-vibration excitations", *Smart Mater. Struct.*, **20**(10), 105029.
- Ying, Z.G, Wang, Y., Ni, Y.Q. and Ko, J.M. (2009), "Stochastic response analysis of piezoelectric axisymmetric hollow cylinders", *J. Sound Vib.*, **321**(3-5), 735-761.
- Ying, Z.G. and Zhu, X.Q. (2009), "Response analysis of piezoelectric shells in plane strain under random excitations", *Acta Mech. Solida Sin.*, **22**, 152-160.
- Yu, L.Y. and Giurgiutiu, V. (2005), "Advances signal processing for enhanced damage detection with piezoelectric wafer active sensors", *Smart Struct. Syst.*, **1**(2), 185-215.
- Zeng, X.W. (2006), "Applications of piezoelectric sensors in geotechnical engineering", *Smart Struct. Syst.*, **2**(3), 237-251.